Steric Influence on the Reactivity of Silyl-*o*-carboranes: Oxidative-Addition Reactions Involving Si−H and B−H Activation

Young-Joo Lee,† Jong-Dae Lee,† Sung-Joon Kim,† Jaejung Ko,*,† Il-Hwan Suh,† Minserk Cheong,*,‡ and Sang Ook Kang*,†

Department of Chemistry, Korea University, 208 Seochang, Chochiwon, Chung-nam 339-700, Korea, and Department of Chemistry and Research Institute for Basic Sciences, Kyung Hee University, Seoul 130-701, Korea

Received September 25, 2003

The reactivity of mono(silyl)- and bis(silyl)-*o*-carboranes $(HSiR_2)_n(C_2B_{10}H_{12-n})$ (n = 1, R = Me, **1a**; n = 1, R = Et, **1b**; n = 2, R = Me, **3a**; n = 2, R = Et, **3b**) toward six-coordinate iridium $[(Cp^*IrCl_2)_2]$ and nine-coordinate rhenium $[ReH_7(PPh_3)_2]$ complexes has been investigated. Reactions between the mono(silyl)-*o*-carboranes (**1a**,**b**) and $(Cp^*IrCl_2)_2$ resulted in the formation of four-membered, cyclic seven-coordinate iridium complexes $Cp^*IrH_2[\eta^1:\eta^1\text{-}(SiR_2)BC_2B_9H_{10}\text{-}Si,B]$ (R = Me, **2a**; R = Et, **2b**), where Si−H activation in the mono(silyl)-*o*-carborane (**1**) is accompanied by the concomitant B−H activation of a neighboring boron hydride. The X-ray structure of **2a** reveals that the iridium center is coordinated to both silicon and boron in a four-legged piano-stool arrangement. In the reaction between the bis(silyl)-*o*-carboranes (**3a**,**b**) and $(Cp^*IrCl_2)_2$, silylation occurs at both Si−H sites, giving rise to the complexes $Cp^*IrH_2[\eta^1:\eta^1\text{-}(SiR_2)_2C_2B_{10}H_{10}\text{-}Si,Si']$ (R = Me, **4a**; R = Et, **4b**), in which the metal center forms part of a five-membered metallacycle (Ir−Si−C−C−Si). Interestingly, the reaction of **3a** with $ReH_7(PPh_3)_2$ afforded the kinetically stabilized intermediate $(PPh_3)_2ReH_5[\eta^1\text{-}SiMe_2C_2B_{10}H_{10}(SiMe_2H)\text{-}Si]$ (**8**), in which only one of the Si−H groups is coordinated, as determined by X-ray crystallography.

Introduction

The synthesis and study of organometallic complexes possessing ancillary silyl-*o*-carboranyl ligands has received considerable attention in the chemistry of group 10 metals, due mainly to its ability to impart a high degree of kinetic stability to its complexes.[1] We have previously reported that the bis(silyl)-*o*-carborane reacts with group 10 metal compounds to yield stable cyclic bis(silyl)metal complexes,[2] which have been identified as key intermediates in the metal-catalyzed double silylation of alkynes,[3] alkenes,[4] nitriles,[5] and aldehydes.[6] In particular, the platinum complex $(PPh_3)_2Pt[\eta^1:\eta^1\text{-}(SiMe_2)_2C_2B_{10}H_{10}\text{-}Si,Si']$ exhibits an unusually high kinetic stability, which has been attributed to the unique electronic and steric effects of the *o*-carborane moiety and the strengthening of the Pt−Si bond.

As a continuation of our work, we now describe the oxidative addition reactions between the mono- and disubstituted silyl-*o*-carboranes (**1**, **3**) and six-coordinate iridium $[(Cp^*IrCl_2)_2]$ and nine-coordinate rhenium $[ReH_7(PPh_3)_2]$ metal complexes. We have been able to demonstrate that the bulkiness of the ancillary *o*-carboranyl group in the silyl ligands $(HSiR_2)_n(C_2B_{10}H_{12-n})$ (**1**, **3**) plays an important role in the Si−H and B−H activation processes (Chart 1). In the reaction between $(Cp^*IrCl_2)_2$ and **1**, Si−H activation results in the formation of a monosilylated complex, in which the ancillary *o*-carboranyl group is drawn sufficiently close to the iridium center to initiate B−H activation, affording the corresponding cyclometalated species $Cp^*IrH_2[\eta^1:\eta^1\text{-}(SiR_2)BC_2B_9H_{10}\text{-}Si,B]$ (R = Me, **2a**; R = Et, **2b**). Interestingly, the analogous (bis)silyl compound **3** undergoes double-silylation reactions at the iridium metal to afford the chelated $Cp^*IrH_2[\eta^1:\eta^1\text{-}(SiR_2)_2C_2B_{10}H_{10}\text{-}Si,Si']$ (R = Me, **4a**; R = Et, **4b**) complex. In the reaction between **3a** and $ReH_7(PPh_3)_2$, oxidative addition affords an intermediate complex, in which the potentially chelating (bis)silyl compound is bound to the rhenium center through just one silyl group, as confirmed by X-ray crystallography. Thus, mono- and disubstituted silyls comprising a bulky *o*-carborane backbone have been

* To whom correspondence should be addressed. Tel: +82-41-860-1334. Fax: +82-41-867-5396. E-mail: sangok@korea.ac.kr.
† Korea University.
‡ Kyung Hee University.

(1) Review: (a) Kang, S. O.; Ko, J. *Adv. Organomet. Chem.* **2001**, *47*, 66. (b) Kang, S. O.; Lee, J.; Ko, J. *Coord. Chem. Rev.* **2002**, *231*, 47.

(2) (a) Kang, Y.; Lee, J.; Kong, Y. K.; Kang, S. O.; Ko, J. *Organometallics* **2000**, *19*, 1722. (b) Kang, Y.; Kang, S. O.; Ko, J. *Organometallics* **2000**, *19*, 1216. (c) Kang, Y.; Kang, S. O.; Ko, J. *Organometallics* **1999**, *18*, 1818. (d) Kang, Y.; Lee, J.; Kong, Y. K.; Kang, S. O.; Ko, J. *Chem. Commun.* **1998**, 2343.

(3) (a) Naka, A.; Okazaki, S.; Hayashi, M.; Ishikawa, M. *J. Organomet. Chem.* **1995**, *499*, 35. (b) Ishikawa, M.; Ohshita, J.; Ito, Y. *Organometallics* **1986**, *5*, 1518. (c) Ishikawa, M.; Matsuzawa, S.; Higuchi, T.; Kamitori, S.; Hirotsu, K. *Organometallics* **1985**, *4*, 2040. (d) Ishikawa, M.; Matsuzawa, S.; Hirotsu, K.; Kamitori, S.; Higuchi, T. *Organometallics* **1984**, *3*, 1930. (e) Kiso, Y.; Tamao, K.; Kumada, M. *J. Organomet. Chem.* **1974**, *76*, 105.

(4) Ishikawa, M.; Okazaki, S.; Naka, A.; Tachibana, A.; Kawauchi, S.; Yamabe, T. *Organometallics* **1995**, *14*, 114.

(5) Reddy, N. P.; Uchimaru, Y.; Lautenschlager, H.-J.; Tanaka, M. *Chem. Lett.* **1992**, 45.

(6) Uchimaru, Y.; Lautenschlager, H.-J.; Wynd, A. J.; Tanaka, M.; Goto, M. *Organometallics* **1992**, *11*, 2639.

10.1021/om034194d CCC: $27.50
Publication on Web 12/06/2003

Chart 1. Mono- and Bis(silyl)metal Complexes Depicting both Si−H and B−H Activation

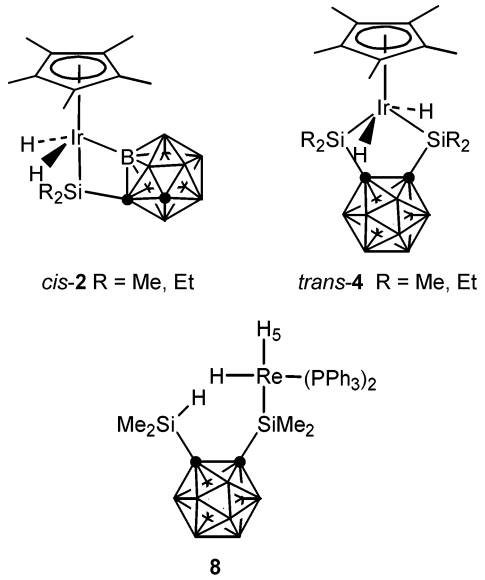

Scheme 1. Formation of the Cyclometalate 2 through Si−H and B−H Activation of the Mono(silyl)-*o*-carborane 1[a]

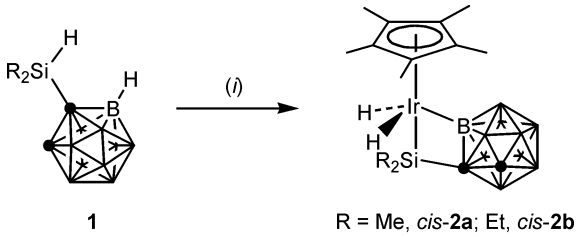

[a] Conditions: (i) ½ $(Cp^*IrCl_2)_2$, NEt_3, THF, 25 °C.

further exploited in chemical transformations such as Si−H and B−H activation, as shown in Chart 1.

Results and Discussions

Reaction of the Mono(silyl)-*o*-carborane with $(Cp^*IrCl_2)_2$. When the mono(silyl) ligand **1** is stirred with $(Cp^*IrCl_2)_2$ at room temperature (2 h), the mutually cis Si−H and B−H groups undergo consecutive activation to afford the corresponding cyclometalates **2**, as shown in Scheme 1. This reaction was found to occur only in the presence of base (triethylamine), where a series of color changes, from orange to yellow and finally colorless, support the gradual formation of the cyclometalate **2**.

The first indication of successful cyclometalation in **2a**,**b** is the appearance of singlet resonances in the $^{11}B\{^1H\}$ NMR spectrum at −22.38 and −22.03 ppm, respectively, which are characteristic of metal-bonded borons.[7] As expected, once the rigid iridasilacycle is formed, the individual borons of the *o*-carborane ligand become chemically and magnetically inequivalent, giving rise to 10 distinct signals in the $^{11}B\{^1H\}$ NMR spectrum. Importantly, this alteration in the stereochemistry also causes the silicon-bound alkyl groups to become nonequivalent, as confirmed by the occurrence of the following signals in the relevant NMR spectra:

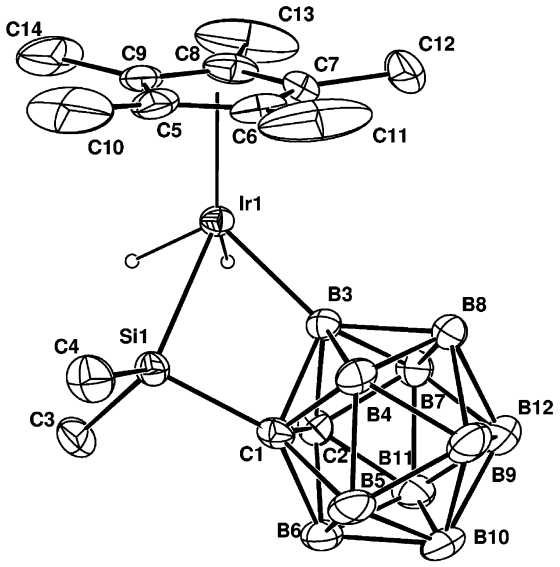

Figure 1. Molecular structure of **2a** with thermal ellipsoids drawn at the 30% level.

^1H, two singlets at δ 0.36 and 0.49 for **2a** and a multiplet at δ 0.86−0.99 for **2b**; $^{13}C\{^1H\}$, two singlets at δ 5.07 and 5.46 for **2a** and four singlets at around δ 4.72−7.92 for **2b**. To further corroborate the NMR spectral data, the X-ray structural analysis of **2a** proves beyond doubt the existence of a cyclometalated silyl ligand.

The coordination geometry around the Ir center in **2a** (Figure 1; selected bond distances and angles are given in Tables 2 and 3, respectively) is a distorted-square-pyramidal arrangement, formed by the Cp* ring, the silyl and boron groups of the metalated *o*-carboranyl ligand, and the two hydrides. The positions of the hydrides were determined from difference maps but were not refined. The four-membered iridasilacycle of **2a** shows a slight folding along the B(1)−Si(1) vector, which is probably due to the greater steric crowding around the iridium metal center. This steric crowding is reflected in the dihedral angle (0.6(4)°) formed between the [Ir(1), B(3), Si(1)] and [C(1), B(3), Si(1)] planes. In addition, the iridacyclic ring [Ir(1), B(3), Si(1)] is tilted by 52.4(2)° relative to the Cp* ring, which in turn influences the positions of the two hydrides, which most likely occupy the vacant locations opposite the iridacycle in a cisoid fashion. The Ir−Si bond distance is relatively long (2.380(2) Å) compared to the same bond in the noncyclometalated complex **6** (2.357(1) Å). As in similar cyclometalated *o*-carboranyl complexes,[8] a certain amount of strain is evident within the four-membered ring, such that the associated bond angles are distorted from their ideal geometries: B(3)−Ir(1)−Si(1) = 68.0(2)° instead of 90°; Ir(1)−B(3)−C(1) = 110.4(4)° instead of 120°; B(3)−C(1)−Si(1) = 87.1(3)° instead of 120°; C(1)−Si(1)−Ir(1) = 94.5(2)° rather than the ideal tetrahedral angle.

We postulate that the formation of **2** probably involves the initial oxidative addition of $HSiR_2(C_2B_{10}H_{11})$ (**1**) to $(Cp^*IrCl_2)_2$, followed by the subsequent release of the $ClSiR_2(C_2B_{10}H_{11})$ byproduct and hydride intermediates of the type $(Cp^*Ir)_2H_nCl_{4-n}$. Successive addition of **1** to these intermediate hydrides eventually leads

(7) Hoel, E. L.; Hawthorne, M. F. *J. Am. Chem. Soc.* **1974**, *96*, 6770.

(8) Bae, J.-Y.; Lee, Y.-J.; Kim, S.-J.; Ko, J.; Cho, S.; Kang, S. O. *Organometallics* **2000**, *19*, 1514.

Table 1. X-ray Crystallographic Data and Processing Parameters for Compounds 2a, 6, 8, and 9·2C$_7$H$_8$

	2a	**6**	**8**	**9**·2C$_7$H$_8$
formula	$B_{10}C_{14}H_{33}SiIr$	$C_{20}H_{33}Si_2Ir$	$B_{10}C_{42}H_{59}Si_2P_2Re$	$B_{10}C_{56}H_{73}Si_2P_2Re$
fw	529.79	521.84	976.31	1158.61
cryst class	orthorhombic	triclinic	triclinic	monoclinic
space group	*Pbca*	$P\bar{1}$	$P\bar{1}$	*C*2/*c*
Z	8	2	2	8
cell constants				
a, Å	19.223(1)	9.205(1)	11.3828(9)	33.296(2)
b, Å	16.73780(9)	10.5230(6)	14.350(2)	12.581(2)
c, Å	13.7827(9)	12.7868(8)	16.218(2)	27.983(1)
α, deg		107.819(5)	66.73(1)	
β, deg		91.172(7)	82.686(9)	94.285(4)
γ, deg		109.873(7)	71.599(8)	
V, Å^3	4434.5(4)	1098.2(2)	2309.3(5)	11689(2)
μ, mm^{-1}	6.072	6.187	2.782	2.210
cryst size, mm	0.4 × 0.4 × 0.5	0.5 × 0.55 × 0.55	0.3 × 0.4 × 0.4	0.30 × 0.30 × 0.30
d_{calcd}, g/cm^3	1.587	1.578	1.404	1.311
F(000)	2064	516	988	4696
radiation		Mo Kα (λ = 0.7107)		
θ range, deg	2.12−25.96	1.69−25.97	1.37−25.97	1.23−25.97
h, *k*, *l* collected	0−23, 0−20, 0−16	0−11, −12 to +12, −15 to +15	0−14, −17 to +17, −19 to +19	−40 to +40, −15 to +7, −34 to +34
no. of rflns measd	4385	4616	9553	23 011
no. of unique rflns	4348	4295	9035	11 454
no. of rflns used in refinement ($I > 2\sigma(I)$)	3040	3890	3840	5743
no. of params	254	223	535	572
R1[a] ($I > 2\sigma(I)$)	0.0318	0.0225	0.1141	0.0619
wR2[a] (all data)	0.0747	0.0562	0.3477	0.2208
GOF	1.072	1.093	0.974	0.962

[a] R1 = $\sum||F_o| - |F_c||$ (based on reflections with $F_o^2 > 2\sigma F^2$). wR2 = $[\sum[w(F_o^2 - F_c^2)^2]/\sum[w(F_o^2)^2]]^{1/2}$; $w = 1/[\sigma^2(F_o^2) + (0.095P)^2]$; $P = [\max(F_o^2, 0) + 2F_c^2]/3$ (also with $F_o^2 > 2\sigma F^2$).

Table 2. Selected Interatomic Distances (Å) for Compounds 2a, 6, 8, and 9·2C$_7$H$_8$

Compound **2a**									
Ir(1)−Si(1)	2.380(2)	Ir(1)−B(3)	2.109(6)	Si(1)−C(1)	1.915(6)	Ir(1)−C(5)	2.269(7)	Ir(1)−C(6)	2.267(6)
Ir(1)−C(7)	2.251(5)	Ir(1)−C(8)	2.265(6)	Ir(1)−C(9)	2.270(7)	Si(1)−C(3)	1.864(6)	Si(1)−C(4)	1.863(6)
Compound **6**									
Ir(1)−Si(1)	2.359(1)	Ir(1)−Si(2)	2.355(1)	Si(1)−C(2)	1.896(4)	Si(2)−C(1)	1.890(5)	Ir(1)−C(11)	2.261(4)
Ir(1)−C(12)	2.252(4)	Ir(1)−C(13)	2.253(4)	Ir(1)−C(14)	2.291(4)	Ir(1)−C(15)	2.265(4)	Si(2)−C(10)	1.892(5)
Si(1)−C(7)	1.875(4)	Si(1)−C(8)	1.877(4)	Si(2)−C(9)	1.892(4)				
Compound **8**									
Re(1)−Si(1)	2.449(5)	Re(1)−P(1)	2.438(6)	Re(1)−P(2)	2.463(6)	Si(1)−C(1)	2.01(2)	Si(2)−C(2)	1.86(3)
P(1)−C(7)	1.86(2)	P(1)−C(13)	1.83(2)	P(1)−C(19)	1.83(2)	P(2)−C(25)	1.82(3)	P(2)−C(31)	1.81(2)
P(2)−C(37)	1.83(3)	Si(1)−C(3)	1.86(2)	Si(1)−C(4)	1.80(3)	Si(2)−C(5)	2.01(7)	Si(2)−C(6)	1.83(4)
Compound **9**·2C$_7$H$_8$									
Re(1)−P(2)	2.464(3)	Re(1)−P(1)	2.466(3)	Re(1)−Si(2)	2.475(3)	P(2)−C(25)	1.852(1)	Si(1)−C(4)	1.85(1)
Re(1)−Si(1)	2.477(3)	P(1)−C(7)	1.81(1)	P(1)−C(13)	1.83(1)	Si(1)−C(1)	1.94(1)	Si(2)−C(6)	1.87(1)
P(1)−C(19)	1.85(1)	P(2)−C(31)	1.81(1)	P(2)−C(37)	1.83(1)	Si(2)−C(2)	1.95(1)	Si(1)−C(3)	1.86(1)

to the formation of **2**. A similar mechanism has previously been proposed for the formation of $(Cp^*Ir)_2H_2(SiR_3)_2$.[9]

Theoretical studies involving geometry optimization have proven to be efficient in locating hydride positions in transition-metal complexes.[10] Here, we have assigned the hydride positions in complex **2a** using density functional theory (DFT) calculations, where those occupying a cisoid disposition are calculated to be more stable than those with a transoid disposition, by 3.7 kcal/mol. The optimized cisoid structure of **2a** is presented in Figure 2, along with a summary of the most significant geometrical parameters. The main structural features of the calculated geometry of **2a** are in good agreement with those determined by X-ray crystallographic methods. From the DFT calculations, we can confirm that the structure of **2a** fits quite neatly with the pseudo-square-pyramidal geometry of the model ML_5 complex. The calculated H−H distance (1.745 Å) between the two hydrides of complex **2a,** coupled with the H−Si (2.296 Å) and H−B (2.114 Å) distances, all suggest that complete oxidative addition of the Si−H and B−H units to the iridium center has occurred.

To our knowledge, complexes **2a**,**b** are the first examples of metallacyclobutanes formed through cyclometalation with one of the B−H units of a mono(silyl)-*o*-carborane. The use of a base in the cyclometalation of **2** is noteworthy, since it clearly indicates that its presence is necessary to initiate intramolecular B−H activation in *o*-carboranes. Similarly, it has been noted that metalation (proceeded by a series of rearrangements) of the analogous *o*-carboranedithiolate Cp*Ir[η^1:η^1-$S_2C_2B_{10}H_{10}$-*S*,*S*′] via B−H activation, was found to proceed at ambient temperatures and below, in the presence of activated acetylenes.[8]

(9) (a) Fernandez, M.-J.; Bailey, P. M.; Bentz, P. O.; Ricci, J. S.; Koetzle, T. F.; Maitlis, P. M. *J. Am. Chem. Soc.* **1984**, *106*, 5458. (b) Fernandez, M.-J.; Bailey, P. M.; Fernandez, M.-J.; Maitlis, P. M. *Organometallics* **1983**, *2*, 164.

(10) Lin, Z.; Hall, M. B. *Coord. Chem. Rev.* **1994**, *135/136*, 845 and references therein.

Table 3. Selected Interatomic Angles (deg) for Compounds 2a, 6, 8, and 9·2C$_7$H$_8$

Compound **2a**							
Si(1)−Ir(1)−B(3)	68.0(2)	Ir(1)−B(3)−C(1)	110.4(4)	B(3)−C(1)−Si(1)	87.1(3)	C(1)−Si(1)−Ir(1)	94.5(2)
C(3)−Si(1)−C(4)	106.3(3)	Ir(1)−Si(1)−C(3)	119.5(2)	Ir(1)−Si(1)−C(4)	119.4(2)	Ir(1)−B(3)−B(8)	137.9(4)
Ir(1)−B(3)−B(4)	120.5(4)	Ir(1)−B(3)−C(2)	119.6(4)				
Compound **6**							
Si(1)−Ir(1)−Si(2)	88.44(4)	Ir(1)−Si(1)−C(2)	105.8(1)	Si(1)−C(2)−C(1)	120.0(3)	C(2)−C(1)−Si(2)	119.4(3)
C(1)−Si(2)−Ir(1)	106.4(1)	Ir(1)−Si(1)−C(7)	115.5(2)	Ir(1)−Si(1)−C(8)	115.6(2)	Ir(1)−Si(2)−C(9)	114.8(2)
Ir(1)−Si(2)−C(10)	114.1(2)						
Compound **8**							
P(1)−Re(1)−P(2)	105.9(2)	P(1)−Re(1)−Si(1)	128.1(2)	P(2)−Re(1)−Si(1)	125.8(2)	Re(1)−Si(1)−C(1)	116.0(7)
Re(1)−Si(1)−C(3)	114.4(7)	Re(1)−Si(1)−C(4)	116.1(9)	Re(1)−P(1)−C(7)	117.1(8)	Re(1)−P(1)−C(13)	112.1(8)
Re(1)−P(1)−C(19)	117.7(9)	Re(1)−P(2)−C(25)	113.9(8)	Re(1)−P(2)−C(31)	119.5(8)	Re(1)−P(2)−C(37)	116.2(9)
Si(1)−C(1)−C(2)	124(2)	C(1)−C(2)−Si(2)	125(2)				
Compound **9**·2C$_7$H$_8$							
P(2)−Re(1)−P(1)	98.8(1)	P(2)−Re(1)−Si(2)	117.0(1)	P(1)−Re(1)−Si(2)	110.9(1)	C(4)−Si(1)−Re(1)	116.3(5)
P(2)−Re(1)−Si(1)	126.9(1)	P(1)−Re(1)−Si(1)	115.8(1)	Si(2)−Re(1)−Si(1)	87.8(1)	C(3)−Si(1)−Re(1)	116.8(5)
C(7)−P(1)−Re(1)	111.6(4)	C(13)−P(1)−Re(1)	118.8(5)	C(19)−P(1)−Re(1)	118.6(4)	C(5)−Si(2)−Re(1)	116.5(5)
C(31)−P(2)−Re(1)	116.4(4)	C(37)−P(2)−Re(1)	118.1(4)	C(25)−P(2)−Re(1)	113.4(4)	C(6)−Si(2)−Re(1)	116.9(5)
C(1)−Si(1)−Re(1)	109.3(4)	C(2)−Si(2)−Re(1)	109.6(3)				

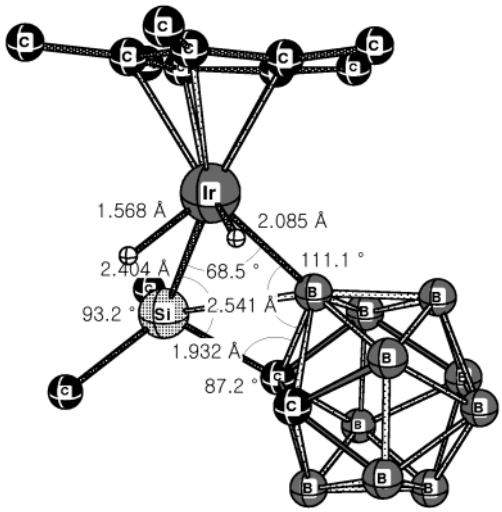

Figure 2. DFT optimized structure of **2a** with important structural parameters.

Scheme 2. Formation of the Stable Bis(silyl)iridium Complex 4[a]

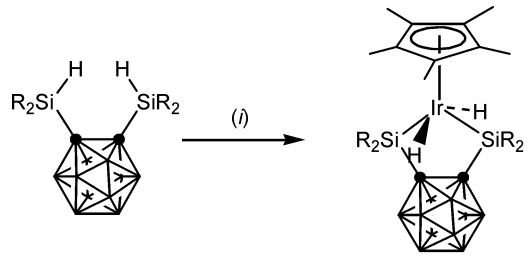

3 R = Me, *trans*-**4a**; Et, *trans*-**4b**

[a] Conditions: (i) $^1/_2$ (Cp*IrCl$_2$)$_2$, NEt$_3$, THF, 25 °C.

Synthesis of the Disilacycloiridium Complex 4. The disilacycloiridium complexes **4** were conveniently prepared (44−62%) by reacting (Cp*IrCl$_2$)$_2$ with bis(silyl)-*o*-carborane (**3**) in THF, in the presence of triethylamine at 25 °C (2 h) (Scheme 2). Chromatographic separation of the crude product afforded large, colorless plates, which are freely soluble in hydrocarbon solvents and stable to air. We believe that **4** arises from the reaction between **3** and (Cp*IrCl$_2$)$_2$ in a manner similar to that reported for the formation of [Cp*Ir(H)$_2$(SiEt$_3$)$_2$] from HSiEt$_3$ and (Cp*IrCl$_2$)$_2$.[9]

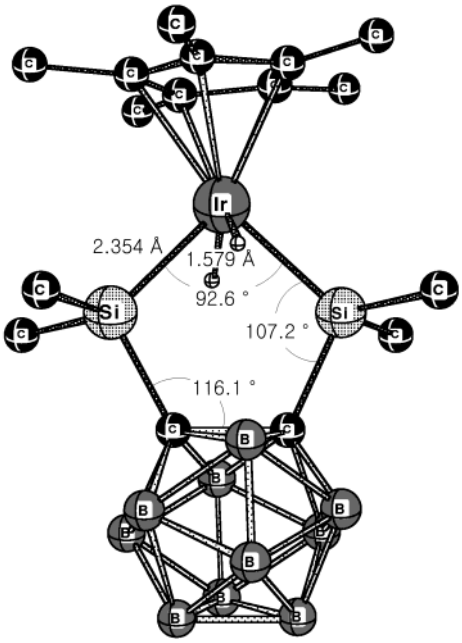

Figure 3. DFT optimized structure of **4a** with important structural parameters.

The ^{1}H NMR spectra of complexes **3a**,**b** exhibit signals confirming the presence of η^5-C$_5$Me$_5$, alkylsilyl, and hydride groups. The corresponding signal integrals, together with elemental analysis results, suggest the formation of a complex of formula Cp*IrH$_2$[η^2-(SiR$_2$)$_2$-C$_2$B$_{10}$H$_{10}$-*Si,Si'*]. An FT-IR study of complex **4** reveals weak ν(Ir−H) bands at 2166 cm^{-1} with peak intensities similar to those observed for Cp*IrH$_2$(SiEt$_3$)$_2$ (2135 cm^{-1}).[11] To examine the stabilizing influence of the chelating bis-silylated carboranyl on **4**, we performed a series of density functional calculations on the model complex **4a**, the optimized structure of which is shown, along with some of its important structural parameters, in Figure 3. Notably, the DFT calculations reveal that the transoid disposition of hydride ligands is more stable

(11) Fernandez, M.-J.; Maitlis, P. M. *J. Chem. Soc., Dalton Trans.* **1984**, 2063.

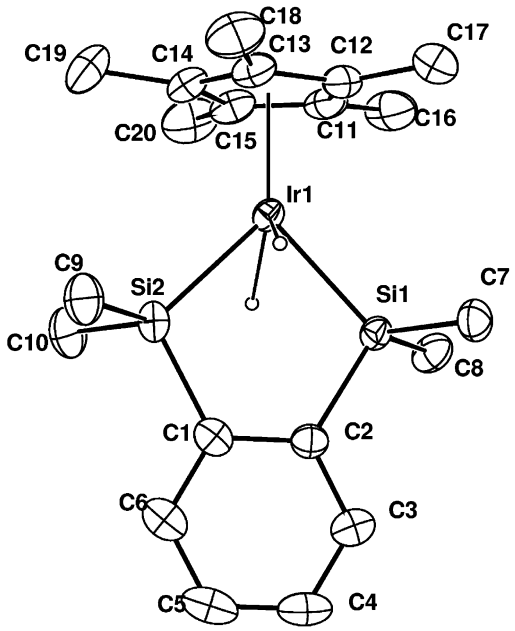

Figure 4. Molecular structure of **6** with thermal ellipsoids drawn at the 30% level.

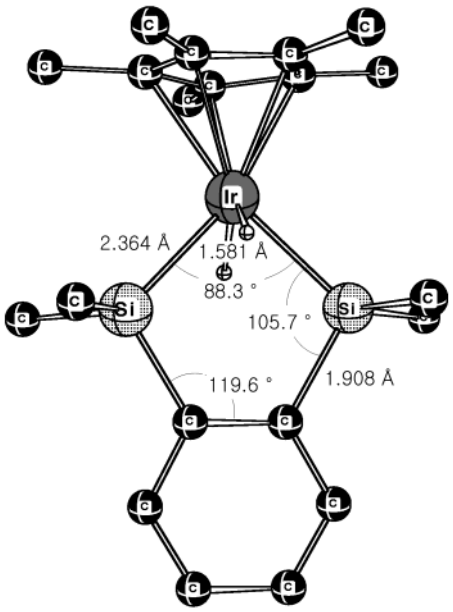

Figure 5. DFT optimized structure of **6** with important structural parameters.

than the cisoid structure by 9.2 kcal/mol (see the Supporting Information).

To verify the significance of the bis-silylated *o*-carboranyl ligand, we performed a similar reaction between $(Cp^*IrCl_2)_2$ and the analogous bis(silyl)benzene **5**, as shown in eq 1.

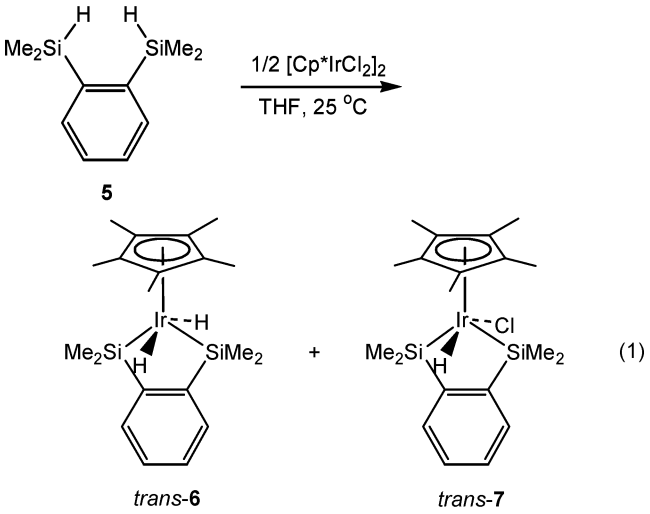

(1)

In addition to the expected bis-silylated product **6**, we observed the second bis-silylated species **7**, toward the end of the reaction, which was isolated in a ca. 1:1.5 ratio with **6**. The X-ray crystallographic determination of **6** at room temperature (Figure 4) revealed a four-legged piano-stool geometry, in which the silyl and hydride ligands are transoid. The positions of the hydrides were determined from difference maps. The metal−silicon and metal−hydrogen bond lengths and angles are similar to the values reported for the corresponding $Cp^*MH_2(SiEt_3)_2$ (M = Rh, Ir) complexes.[12,13]

The structural analysis of the η^5-bonded C_5Me_5 ring (average Ir−C = 2.264(4) Å) reveals a uniformity within the ring carbon−carbon bonds (average C−C = 1.428(7) Å), implying it has an undistorted conformation. The ring is bisected by a mirror plane containing the hydrides (average Ir−H = 1.649 Å), in which the two dimethylsilyl ligands are reflected (Ir−Si = 2.357(1) Å). The Ir−Si bond length is comparable with the same bond lengths reported for the octahedral and pentacoordinate Ir(III) complexes, as well as the Ir−Si bond distance reported for the seven-coordinate Ir(V) silyls.[11,14] The complexes may therefore be defined as possessing a total of five formally uninegative ligands about the iridium center, giving the metal a formal +5 oxidation state. Using DFT calculations, we observed that complex **6** is more stable in the transoid rather than cisoid disposition of hydrides, by 5.8 kcal/mol (see the Supporting Information). The optimized structure of **6** is shown along with some of its major structural parameters in Figure 5.

For unequivocal characterization, we also attempted the X-ray structural determination of **7**. However, poorly diffracting crystals precluded a satisfactory analysis (see the Supporting Information). Nevertheless, the structural data were sufficient to establish that the iridium metal adopts the expected "four-legged piano stool" geometry, as defined by the two silyl groups of the chelated bis(silyl)-*o*-carborane (**3**), a single hydride, and the appearance of a chloride ligand. It is worthy of note that the ligand arrangement in complex **7** is similar to that found in the dihydride complex **6**. Interestingly, the difference between complexes **4** and **7** is even more

(12) (a) Fernandez, M.-J.; Bailey, P. M.; Bentz, P. O.; Ricci, J. S.; Koetzle, T. F.; Maitlis, P. M. *J. Am. Chem. Soc.* **1984**, *106*, 5458. (b) Ricci, J. S.; Koetzle, T. F.; Fernandez, M.-J.; Maitlis, P. M.; Green, J. C. *J. Organomet. Chem.* **1986**, *299*, 383.

(13) (a) Schubert, U.; Müller, J.; Alt, H. G. *Organometallics* **1987**, *6*, 469. (b) Matarossa-Tchiroukhine, E.; Jaouen, G. *Can. J. Chem.* **1988**, *66*, 2157.

(14) (a) Tilley, T. D. In *The Silicon-Heteroatom Bond*; Patai, S., Rappoport, Z., Eds.; Wiley: New York, 1991; pp 264, 343. (b) Goikhman, R.; Aizenberg, M.; Kraatz, H.-B.; Milstein, D. *J. Am. Chem. Soc.* **1995**, *117*, 5865. (c) Aizenberg, M.; Milstein, D. *J. Am. Chem. Soc.* **1995**, *117*, 6456. (d) Tanke, R. S.; Crabtree, R. H. *Organometallics* **1991**, *10*, 415. (e) Loza, M.; Faller, J. W.; Crabtree, R. H. *Inorg. Chem.* **1995**, *34*, 2937. (f) Esteruelas, M. A.; Lahoz, F. J.; Oñate, E.; Oro, L. A.; Rodriguez, L. *Organometallics* **1996**, *15*, 823.

fascinating, since in the latter only the planar phenylene unit is involved in metalation. From the evidence to date, we can infer that **6** and **7** (as well as their precursor **5**) are less sterically congested than their *o*-carborane counterpart **4**, since their planar five-membered rings take up smaller volume, resulting in less strain on the bis(silyl)iridium center. Consequently, the coordination of a chloride ligand in **7** might be the result of the steric constraints imposed by the planar phenylene backbone. It was noted that a decrease in the steric bulk at the bis(silyl)iridium center allows a greater number of chlorides access to the coordination sites. By comparison with the parent ligands **3a** and **5**, the values derived from DFT calculations suggest the structure of **4a** is preferred to **6** by some 7.9 kJ/mol (see the Supporting Information). From a qualitative standpoint, computational calculations derived for complex **4a** are consistent with the corresponding experimental results in that the *o*-carboranyl derivative **4** has been readily prepared without the formation of side products.

Isolation of a Kinetically Stabilized Mono-Silylated Rhenium Hydride (9). The oxidative addition of Si−H to transition-metal polyhydrides is a well-established area of study,[15] particularly when chelating bis-silylated compounds are involved.[16] In the case of the reaction between the chelating bis(silyl)benzene (**5**) and $ReH_7(PPh_3)_2$, an intermediate complex was isolated in which only one Re−Si bond was evident. While the structural details of this species have so far remained elusive, we propose that, by replacement of the phenyl group in **5** with the more bulky *o*-carboranyl unit, it might be possible to produce an intermediate analogue that would be sufficiently more stable to allow a more definitive structural analysis. We feel the bis(silyl)-*o*-carborane **3** is a most promising candidate for this purpose, on the grounds that **3** is sterically more protecting than the corresponding arylsilane **5**. In fact, **3** has been successfully employed in the isolation of several key intermediates obtained from double-silylation reactions, such as L_2M [η^1:η^1-$(SiR_2)_2C_2B_{10}H_{10}$-*Si,Si*] (M = Pt, L = PPh_3; M = Ni, L = PEt_3).[2]

Indeed, the analogous reaction between **3a** and $ReH_7(PPh_3)_2$ at room temperature generated an air-stable, microcrystalline solid identical with the intermediate species isolated in the reaction between **5** and $ReH_7(PPh_3)_2$, (Scheme 3).

The ^{1}H NMR spectrum of compound **8** exhibits resonances which confirm the presence of triphenylphosphine (7.14−7.70 ppm), two nonequivalent dimethylsilyl groups (0.38 and 0.83 ppm), and two nonequivalent metal hydride protons (−5.62 and −5.28 ppm ($^2J_{H-H}$ = 19 Hz)). Recrystallization of the crude intermediate $(PPh_3)_2ReH_6$[η^1-$(SiMe_2)C_2B_{10}H_{10}(SiMe_2H)$-*Si*] (**8**) afforded crystals suitable for X-ray structural determination. From the molecular structure of **8** shown in Figure 6, we observe the expected tricapped-trigonal-prismatic structure in which only one of the silyl groups is bound by the metal, confirming the bis(silyl)-*o*-carborane ligand to be essentially monodentate. The precise location of the six hydrides in **8** could not be confirmed by X-ray crystallographic means; however, we propose they are positioned in the axial positions of a tricapped trigonal prism, in accordance with similar structural determinations on $ReH_6(SiPh_3)(PPh_3)_2$.[15d] The ^{1}H/^{13}C NMR results of the mono(silyl)rhenium complex are in complete agreement with the crystal structure of **8** (Figure 6).

Scheme 3. Sequential Silylation Reactions between 3a and $ReH_7(PPh_3)_2$[a]

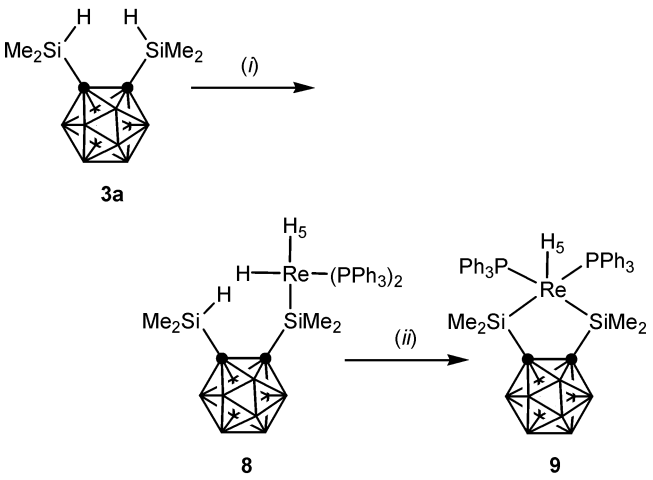

[a] Conditions: (i) $ReH_7(PPh_3)_2$, THF, 25 °C; (ii) toluene, reflux.

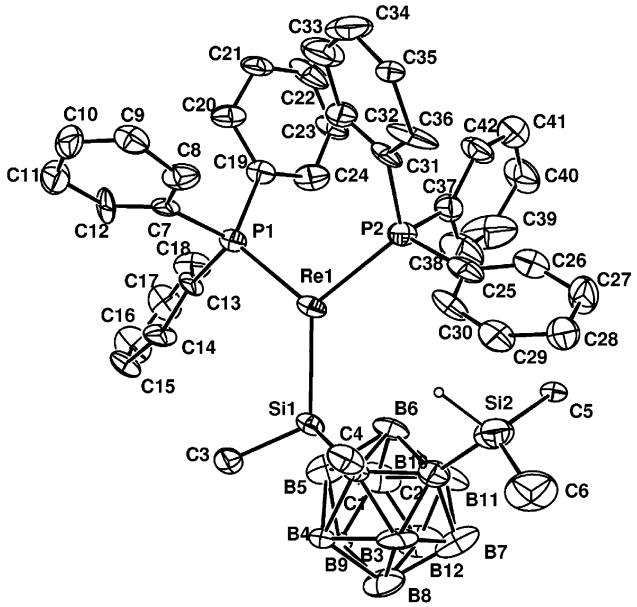

Figure 6. Molecular structure of **8** with thermal ellipsoids drawn at the 30% level.

In an attempt to oxidatively add the remaining Si−H to the rhenium center, a toluene solution of **8** was refluxed for 1 h. Recrystallization of the crude material from toluene afforded the expected cyclic bis(silyl)-rhenium hydride $(PPh_3)_2ReH_5$[η^1:η^1-$(SiMe_2)_2C_2B_{10}H_{10}$-$(SiMe_2H)$-*Si,Si*] (**9**). The composition and stereochemistry of **9** were elucidated from ^{11}B, ^{1}H, and ^{13}C NMR

(15) (a) Delpech, F.; Sabo-Etienne, S.; Donnadieu, B.; Chaudret, B. *Organometallics* **1998**, *17*, 4926. (b) Buil, M.; Espinet, P.; Esteruelas, M. A.; Lahoz, F. J.; Lledós, A.; Martínez-Ilarduya, J. M.; Maseras, F.; Modrego, J.; Oñate, E.; Oro, L. A.; Sola, E.; Valero, C. *Inorg. Chem.* **1996**, *35*, 1250. (c) Takao, T.; Suzuki, H.; Tanaka, M. *Organometallics* **1994**, *13*, 2554. (d) Luo, X.-L.; Baudry, D.; Boydell, P.; Charpin, P.; Nierlich, M.; Ephritikhine, M.; Crabtree, R. H. *Inorg. Chem.* **1990**, *29*, 1511.

(16) (a) Fan, M.-F.; Lin, Z. *Organometallics* **1999**, *18*, 286. (b) Delpech, F.; Sabo-Etienne, S.; Chaudret, B.; Daran, J.-C. *J. Am. Chem. Soc.* **1997**, *119*, 3167. (c) Loza, M.; Faller, J. W.; Crabtree, R. H. *Inorg. Chem.* **1995**, *34*, 2937. (d) Loza, M. L.; de Gala, S. R.; Crabtree, R. H. *Inorg. Chem.* **1994**, *33*, 5073.

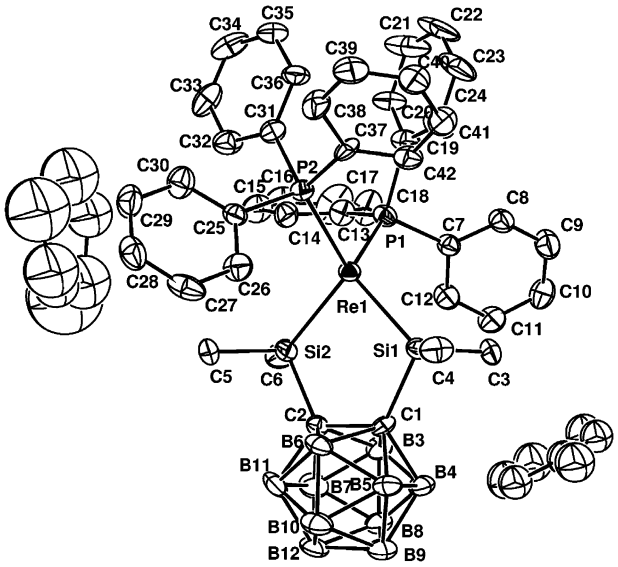

Figure 7. Molecular structure of **9** with thermal ellipsoids drawn at the 30% level.

spectra and elemental analysis data. The multinuclear NMR results of the bis(silyl)rhenium complex are in complete agreement with the crystal structure of **9** (Figure 7). Furthermore, the structure of **9** shows a strong resemblance to that of the previously reported silyl hydride $(PPh_3)_2ReH_5[\eta^1{:}\eta^1\text{-}(SiMe_2)_2C_6H_4\text{-}Si,Si']$,[16d] which adopts a dodecahedral conformation with a transoid disposition of silyls and hydrides.

Summary

The present work reports a series of novel addition reactions via Si−H and B−H activation. Thus, silyl compounds comprising a bulky ancillary *o*-carboranyl backbone have been further exploited in chemical transformations involving Si−H and B−H activation. Because of the presence of a bulky *o*-carboranyl unit, the mono(silyl)-*o*-carborane (**1**) exhibits unusual reactivities which have not been observed in the related complex **5**. For example, the reaction of **1** with six-coordinate $(Cp^*IrCl_2)_2$ affords the cyclometalated products of a coordinated silyl-*o*-carboranyl ligand. The reaction of the bis(silyl)-*o*-carborane **3** with "half-sandwich" six-coordinate iridium complexes produced seven-coordinate iridium hydrides with a four-legged "piano-stool" geometry. The reaction of $ReH_7(PPh_3)_2$ with the chelating bis(silyl)-*o*-carborane (**3a**) also affords an unusual nine-coordinate rhenium product which contains a single silyl group tether.

Experimental Section

General Procedures. All manipulations were performed under a dry, oxygen-free nitrogen or argon atmosphere using standard Schlenk techniques or in a Vacuum Atmospheres HE-493 drybox. Diethyl ether, toluene, hexane, and pentane were distilled under nitrogen from sodium/benzophenone. Dichloromethane was dried with CaH_2. Benzene-d_6 was distilled under nitrogen from sodium and stored in a Schlenk storage flask until needed. $CDCl_3$ was predried under CaH_2 and vacuum-transferred. *n*-BuLi (1.6 M in hexanes) and 1,2-dichlorotetramethyldisilane were used as received from Aldrich. *o*-Carborane was purchased from KATCHEM Ltd. and used without purification. $(Cp^*IrCl_2)_2$[17] and $ReH_7(PPh_3)_2$[18] were prepared according to the literature procedures. All ^1H (300.1 MHz, measured in $CDCl_3$), ^{13}C (75.4 MHz, measured in $CDCl_3$), ^{31}P (121.4 MHz, measured in $CDCl_3$), and ^{29}Si (59.60 MHz, measured in $CDCl_3$) NMR spectra were recorded on a Varian Mercury-300BB spectrometer unless otherwise stated. ^1H and ^{13}C NMR chemical shifts are reported relative to Me_4Si and were determined by reference to the residual ^1H or ^{13}C solvent peaks. Elemental analyses were performed with a Carlo Erba Instruments CHNS−O EA1108 analyzer.

Synthesis of Mono(silyl)-*o*-carborane 1. A representative procedure is as follows: to a solution of 0.72 g (5.0 mmol) of *o*-carborane in 80 mL of THF, precooled to −78 °C, was added 3.13 mL of *n*-butyllithium (1.6 M in hexanes). The reaction mixture was warmed to room temperature and stirred for 2 h, whereupon it was transferred, via cannula, to a suspension of 5.5 mmol (1.1 equiv) of dimethylchlorosilane in 20 mL of Et_2O that was cooled to −78 °C. The resultant yellow mixture was warmed to room temperature and stirred for 2 h. The volatiles were then removed under reduced pressure; the crude mixture was taken up in a minimal amount of Et_2O and filtered through a 1 × 5 cm pad of silica gel on a glass frit. Removal of the volatiles provided the final crude product, which was further purified from toluene at −5 °C to provide pure dimethylsilyl-*o*-carborane **1a** as a colorless oil. Yield: 87% (0.88 g, 4.35 mmol). ^1H NMR: δ 4.10 (m, 1H, Si*H*, $^3J_{H-H} = 4$ Hz), 3.38 (br, 1H, Ccab-*H*), 0.33 (d, 6H, $SiMe_2$, $^3J_{H-H} = 4$ Hz). $^{13}C\{^1H\}$ NMR: δ −3.94 (Si*Me*$_2$). IR (KBr, cm^{-1}): 2983 w, 2977 w (ν_{CH}), 2610 w, 2582 s (ν_{BH}), 2156 w (ν_{SiH}). Anal. Calcd for $B_{10}C_4H_{18}Si$: C, 23.51; H, 8.88. Found: C, 23.43; H, 8.91.

1b. A procedure analogous to the preparation of **1a** was used, but starting from diethylchlorosilane (0.68 g, 5.5 mmol) in benzene. Thus, **1b** was purified from toluene at −5 °C. Yield: 81% (0.93 g, 4.05 mmol). ^1H NMR: δ 3.89 (m, 1H, Si*H*, $^3J_{H-H} = 3$ Hz), 3.38 (br, 1H, Ccab-*H*), 1.06 (t, 6H, $SiCH_2$*Me*, $^3J_{H-H} = 8$ Hz), 0.84 (m, 4H, $SiCH_2$Me). $^{13}C\{^1H\}$ NMR: δ 7.69, 3.22 (Si*Et*$_2$). IR (KBr, cm^{-1}): 2983 w, 2971 w (ν_{CH}), 2587 s (ν_{BH}), 2143 w (ν_{SiH}). Anal. Calcd for $B_{10}C_6H_{22}Si$: C, 13.03; H, 12.03. Found: C, 13.07; H, 12.07.

Synthesis of Bis(silyl)-*o*-carborane 3. A representative procedure is as follows: to a solution of 0.72 g (5.0 mmol) of *o*-carborane in 80 mL of THF, precooled to −78 °C, was added 6.90 mL of *n*-butyllithium (1.6 M in hexanes). The reaction mixture was warmed to room temperature and stirred for 2 h, whereupon it was transferred, via cannula, to a suspension of 11.0 mmol (2.2 equiv) of dimethylchlorosilane in 20 mL of Et_2O that was cooled to −78 °C. The resultant yellow mixture was warmed to room temperature and stirred for 2 h. The solution was reduced in vacuo to about half its orginal volume, and some insoluble material was removed by filtration. The crude residue was purified from toluene at −5 °C to provide pure bis(dimethylsilyl)-*o*-carborane **3a** as a colorless oil. Yield: 89% (1.15 g, 4.45 mmol). ^1H NMR (C_6D_6): δ 4.01 (m, 2H, Si*H*, $^3J_{H-H} = 4$ Hz), −0.03 (d. 12H, Si*Me*$_2$, $^3J_{H-H} = 4$ Hz). $^{13}C\{^1H\}$ NMR (C_6D_6): δ −2.31 (Si*Me*$_2$). IR (KBr, cm^{-1}): 2981 w (ν_{CH}), 2572 s (ν_{BH}) 2554 (ν_{SiH}). Anal. Calcd for $C_6H_{24}B_{10}Si_2$: C, 27.46; H, 9.22. Found: C, 27.55; H, 9.19.

3b. A procedure analogous to the preparation of **3a** was used, but starting from diethylchlorosilane (1.35 g, 5.5 mmol) in benzene. Thus, **3b** was crystallized from toluene at −5 °C. Yield: 83% (1.31 g, 4.15 mmol). ^1H NMR: δ 3.98 (m, 1H, Si*H*, $^3J_{H-H} = 3$ Hz), 1.06 (t, 12H, $SiCH_2$*Me*, $^3J_{H-H} = 7$ Hz), 0.89 (m, 8H, $SiCH_2$Me). $^{13}C\{^1H\}$ NMR: δ 7.83, 4.11 (Si*Et*$_2$). IR (KBr, cm^{-1}): 2993 w, 2975 w (ν_{CH}), 2581 s (ν_{BH}), 2152 w (ν_{SiH}). Anal. Calcd for $B_{10}C_{10}H_{32}Si_2$: C, 37.70; H, 10.13. Found: C, 37.84; H, 10.16.

(17) Kong, J. W.; Moseley, K.; Maitlis, P. M. *J. Am. Chem. Soc.* **1969**, *91*, 5970.
(18) Baudry, D.; Ephritikhine, M.; Felkin, H. *J. Organomet. Chem.* **1982**, *224*, 363.

Reaction of the Mono- or Bis(silyl)-*o*-carborane with $(Cp^*IrCl_2)_2$. A representative procedure is as follows: a 3.0 mmol solution of **1a** in THF (20 mL) was added to a stirred solution of $(Cp^*IrCl_2)_2$ (0.40 g, 0.5 mmol) in THF (30 mL) cooled to −78 °C. A 0.25 g portion of NEt_3 (2.5 mmol) was added with stirring over 30 min. The reaction mixture was then allowed to react at 0 °C for 1 h, and the solution was stirred for another 2 h at room temperature. The solution gradually turned yellow, suggesting the formation of a metal silyl complex. The solution was reduced in vacuo to about half its original volume, and some insoluble material was removed by filtration. The solution was removed under vacuum, and the resulting residue was taken up in a minimum of methylene chloride and then transferred to a column of silica gel. The crude residue was purified by column chromatography, affording >98% pure complex as colorless crystals of **2a**. Yield: 60% (0.079 g, 0.15 mmol). Mp: 163−165 °C dec. ^{1}H NMR: δ 2.91 (br, 1H, Ccab-*H*), 2.13 (s, 15H, C_5Me_5), 0.49 (s, 3H, Si*Me*$_2$), 0.36 (s, 3H, Si*Me*$_2$), −14.88 (br, 1H, Ir−*H*), −14.99 (br, 1H, Ir−*H*). ^{13}C{^{1}H} NMR: δ 98.84 (C_5Me_5), 10.33 (C_5Me_5), 5.46 (Si*Me*$_2$), 5.07 (Si*Me*$_2$). ^{11}B NMR: δ −0.86 (d, 2B, $^1J_{B-H}$ = 150 Hz), −2.62 (d, 2B, $^1J_{B-H}$ = 160 Hz), −8.76 (d, 3B, $^1J_{B-H}$ = 150 Hz), −12.08 (d, 2B, $^1J_{B-H}$ = 150 Hz), −22.38 (s, 1B). ^{29}Si NMR: δ −31.92 (*Si*Me$_2$). IR (KBr, cm^{-1}): 3047 w, 2983 w, 2962 w, 2935 w, 2910 w (ν_{CH}), 2596 s, 2565 s (ν_{BH}), 2187 w, 2165 w (ν_{IrH}). Anal. Calcd for $B_{10}C_{14}H_{33}SiIr$: C, 31.56; H, 6.25. Found: C, 31.67; H, 6.27.

2b. A procedure analogous to the preparation of **2a** was used, but starting from 3.0 mmol of **1b**. After flash chromatography on silica gel with hexane/$CHCl_3$ (90/10), **2b** was isolated as colorless solids. Yield: 53% (0.074 g, 0.13 mmol). Mp: 169−170 °C dec. ^{1}H NMR: δ 2.97 (br, 1H, Ccab-*H*), 2.14 (s, 15H, C_5Me_5), 0.86−0.99 (m, 10H, Si*Et*$_2$), −15.04 (br, 1H, Ir−H_2), −15.37 (br, 1H, Ir−H_2). ^{13}C{^{1}H} NMR: δ 98.85 (C_5Me_5), 10.43 (C_5Me_5), 7.92 (Si*C*H$_2$Me), 7.53 (Si*C*H$_2$Me), 5.57 (SiCH$_2$*Me*), 4.72 (SiCH$_2$*Me*). ^{11}B NMR: δ −0.68 (d, 2B, $^1J_{B-H}$ = 140 Hz), −2.82 (d, 2B, $^1J_{B-H}$ = 140 Hz), −8.50 (d, 3B, $^1J_{B-H}$ = 130 Hz), −12.32 (d, 2B, $^1J_{B-H}$ = 130 Hz), −21.99 (s, 1B). ^{29}Si NMR: δ −21.65 (*Si*Et$_2$). IR (KBr, cm^{-1}): 3045 w, 2991 w, 2959 w, 2943 w, 2910 w (ν_{CH}), 2613 s, 2590 s (ν_{BH}), 2195 w, 2162 w (ν_{IrH}). Anal. Calcd for $B_{10}C_{16}H_{37}SiIr$: C, 34.27; H, 6.66. Found: C, 34.14; H, 6.64.

4a. A procedure analogous to the preparation of **2a** was used, but starting from 3.0 mmol of **3a**. After flash chromatography on silica gel with hexane/$CHCl_3$ (90/10), **4a** was isolated as colorless solids. Yield: 62% (0.091 g, 0.16 mmol). Mp: 181−183 °C dec. ^{1}H NMR: δ 2.10 (s, 15H, C_5Me_5), 0.46 (s, 12H, Si*Me*$_2$), −16.15 (s, 2H, Ir−H_2). ^{13}C{^{1}H} NMR: δ 98.73 (C_5Me_5), 10.45 (C_5Me_5), 5.40 (Si*Me*$_2$). ^{11}B NMR: δ −0.86 (d, 2B, $^1J_{B-H}$ = 140 Hz), −5.37 (d, 2B, $^1J_{B-H}$ = 145 Hz), −10.15 (d, 4B, $^1J_{B-H}$ = 160 Hz), −12.96 (d, 2B, $^1J_{B-H}$ = 140 Hz). ^{29}Si NMR: δ 14.01 (*Si*Me$_2$). IR (KBr, cm^{-1}): 2961 w (ν_{CH}), 2583 s (ν_{BH}), 2166 w (ν_{IrH}). Anal. Calcd for $B_{10}C_{16}H_{39}Si_2Ir$: C, 32.53; H, 6.66. Found: C, 32.43; H, 6.63.

4b. A procedure analogous to the preparation of **2a** was used, but starting from 3.0 mmol of **3b**. After flash chromatography on silica gel with hexane/$CHCl_3$ (90/10), **4b** was isolated as colorless solids. Yield: 44% (0.071 g, 0.11 mmol). Mp: 185−186 °C dec. ^{1}H NMR: δ 2.13 (s, 15H, C_5Me_5), 0.96, −1.17 (m, 20H, Si*Et*$_2$), −15.86 (s, 2H, Ir−H_2). ^{13}C{^{1}H} NMR: δ 98.14 (C_5Me_5), 11.51 (C_5Me_5), 7.83 (Si*C*H$_2$Me), 5.24 (SiCH$_2$*Me*). ^{11}B NMR: δ −2.12 (d, 2B, $^1J_{B-H}$ = 150 Hz), −8.99 (d, 2B, $^1J_{B-H}$ = 150 Hz), −13.60 (d, 4B, $^1J_{B-H}$ = 160 Hz), −14.91 (d, 2B, $^1J_{B-H}$ = 140 Hz). ^{29}Si NMR: δ 30.10 (*Si*Et$_2$). IR (KBr, cm^{-1}): 3069 s, 2963 m, 2874 m (ν_{CH}), 2606 s (ν_{BH}), 2166 w (ν_{IrH}). Anal. Calcd for $B_{10}C_{20}H_{47}Si_2Ir$: C, 37.13; H, 7.33. Found: C, 37.27; H, 7.31.

Reaction of 1,2-Bis(dimethylsilyl)benzene (5) with $(Cp^*IrCl_2)_2$. A 3.0 mmol solution of **5** in THF (20 mL) was added to a stirred solution of $(Cp^*IrCl_2)_2$ (0.40 g, 0.5 mmol) in THF (30 mL) cooled to −78 °C. A 0.253 g portion of NEt_3 (2.5 mmol) was added with stirring over 30 min. The reaction mixture was then allowed to react at 0 °C for 1 h, and the solution was stirred for another 2 h at room temperature. The orange solution turned yellow as the solution warmed. The solution was filtered in air, and the solvent was removed under reduced pressure. The resultant residue was extracted with 60 mL of hexane and reduced to 10 mL. Cooling at −30 °C overnight gave a yellow solid which was dried under vacuum, recrystallized from cold hexane, and characterized as **6** (0.038 g, 0.072 mmol, 29%). Mp: 165−167 °C dec. ^{1}H NMR: δ 7.55 (m, 2H, C_6H_4), 7.18 (m, 2H, C_6H_4), 2.18 (s, 15H, C_5Me_5), 0.53 (s, 12H, Si*Me*$_2$), −16.30 (s, 2H, Ir−H_2). ^{13}C{^{1}H} NMR: δ 131.21, 126.83 (*Ph*), 97.54 (C_5Me_5), 10.69 (C_5Me_5), 6.19 (Si*Me*$_2$). ^{29}Si NMR: δ 1.05 (*Si*Me$_2$). IR (KBr, cm^{-1}): 3040 w, 2980 w, 2963 m, 2937 w (ν_{CH}), 2164 w (ν_{IrH}). Anal. Calcd for $C_{20}H_{33}Si_2Ir$: C, 45.96; H, 6.37. Found: C, 45.80; H, 6.35.

The remaining solid was passed through a short column of silica gel with hexane/$CHCl_3$ (90/10) as the eluent. A 0.060 g (0.011 mmol, 43% yield) amount of **7** was obtained after removal of the solvent. Mp: 172−173 °C dec. ^{1}H NMR: δ 7.52 (m, 2H, C_6H_4), 7.21 (m, 2H, C_6H_4), 1.95 (s, 15H, C_5Me_5), 0.58 (s, 6H, Si*Me*$_2$), 0.55 (s, 6H, Si*Me*$_2$), −16.06 (s, 1H, Ir−*H*). ^{13}C{^{1}H} NMR: δ 131.94, 127.39 (*Ph*), 102.29 (C_5Me_5), 9.72 (C_5Me_5), 7.85 (Si*Me*$_2$), −0.42 (Si*Me*$_2$). ^{29}Si NMR: δ 5.25 (*Si*Me$_2$). IR (KBr, cm^{-1}): 3044 w, 2968 m, 2887 w (ν_{CH}), 2039 w (ν_{IrH}). Anal. Calcd for $C_{20}H_{32}Si_2ClIr$: C, 43.15; H, 5.80. Found: C, 43.29; H, 5.82.

Reaction of 1,2-Bis(dimethylsilyl)-*o*-carborane (3a) with $ReH_7(PPh_3)_2$. Under argon, $ReH_7(PPh_3)_2$ (0.14 g, 0.2 mmol) was added to a stirred solution of complex **3a** (0.052 g, 0.2 mmol) in THF (10 mL) cooled to 0 °C. The pale yellow solution slowly turned dark yellow. After it was stirred for 30 min, the solution was evaporated to dryness. The crude residue was purified from toluene at −5 °C to provide pure silyl-tethered product **8** as yellow crystals. Yield: 0.15 g (0.15 mmol, 75%). Mp: 153−155 °C dec. ^{1}H NMR: δ 7.14−7.70 (m, 30H, P*Ph*$_3$), 4.10 (m, 1H, Si*H*), 0.83 (s, 6H, Si*Me*$_2$), 0.38 (d, 6H, Si*Me*$_2$, $^3J_{H-H}$ = 7 Hz), −5.28 (t, 6H, Re−*H*, $^2J_{H-H}$ = 19 Hz). ^{13}C{^{1}H} NMR: δ 127.82−134.01 (P*Ph*$_3$), 20.85 (Si*Me*$_2$H), −2.35 (Si*Me*$_2$). ^{31}P{^{1}H} NMR: δ 9.95, 23.30 (P*Ph*$_3$). IR (KBr, cm^{-1}): 3053 w, 2978 w (ν_{CH}), 2583 s (ν_{BH}) 1983 w, 1865 w (ν_{ReH}). Anal. Calcd for $B_{10}C_{42}H_{59}Si_2P_2Re$: C, 51.51; H, 6.08. Found: C, 51.70; H, 6.06.

9. A solution of **8** (0.098 g, 0.1 mmol) in toluene (20 mL) was heated for 1 h at 110 °C; conversion into **9**, as monitored by ^{1}H NMR spectroscopy, was quantitative. The solvent was removed in vacuo and the resulting solid crystallized from toluene to give 0.066 g (0.068 mmol) of colorless microcrystals (68% yield). Mp: 166−168 °C dec. ^{1}H NMR: δ 7.08−7.30 (m, 30H, P*Ph*$_3$), 0.35 (s, 12H, Si*Me*$_2$), −6.75 (t, 5H, Re-*H*, $^2J_{H-H}$ = 19 Hz). ^{13}C{^{1}H} NMR: δ 133.66, 133.60, 130.05, 128.02 (P*Ph*$_3$), 13.97 (Si*Me*$_2$). ^{31}P{^{1}H} NMR: δ 23.34 (P*Ph*$_3$). IR (KBr, cm^{-1}): 3057 w, 2957 m (ν_{CH}), 2590 (ν_{BH}), 1981 w, 1867 w (ν_{ReH}). Anal. Calcd for $B_{10}C_{42}H_{57}Si_2P_2Re$: C, 51.62; H, 5.88. Found: C, 51.43; H, 5.86.

Crystal Structure Determination. Crystals of **2a**, **6**, **8**, and **9** were obtained from toluene at −10 °C, sealed in glass capillaries under argon, and mounted on the diffractometer. Data were collected and corrected for Lorentz and polarization effects. Each structure was solved by the application of direct methods using the SHELXS-96 program[19a] and least-squares refinement using SHELXL-97.[19b] After anisotropic refinement of all non-H atoms several H atom positions could be located in difference Fourier maps. These were refined isotropically, while the remaining H atoms were calculated in idealized positions and included into the refinement with fixed atomic contributions. Further detailed information is listed in Table 1.

(19) (a) Sheldrick, G. M. *Acta Crystallogr., Sect. A* **1990**, *A46*, 467. (b) Sheldrick, G. M. SHELXL, Program for Crystal Structure Refinement; University of Göttingen, Göttingen, Germany, 1997.

Computational Details. Stationary points on the potential energy surface were calculated using the Amsterdam Density Functional (ADF) program, developed by Baerends et al.[20,21] and vectorized by Ravenek.[22] The numerical integration scheme applied for the calculations was developed by te Velde et al.[23,24] The geometry optimization procedure was based on the method due to Versluis and Ziegler.[25] The electronic configurations of the molecular systems were described by double-ζ STO basis sets with polarization functions for the H, B, and C atoms, while triple-ζ Slater type basis sets were employed for the Si and Ir atoms.[26,27] The 1s electrons of B and C, the 1s−2p electrons of Si, and the 1s−4d electrons of Ir were treated as frozen cores. A set of auxiliary[28] s, p, d, f, and g STO functions, centered on all nuclei, was used in order to fit the molecular density and the Coulomb and exchange potentials in each SCF cycle. Energy differences were calculated by augmenting the local exchange-correlation potential by Vosko et al.[29] with Becke's[30] nonlocal exchange corrections and Perdew's[31] nonlocal correlation corrections (BP86). Geometries were optimized including nonlocal corrections at this level of theory. First-order Pauli scalar relativistic corrections[32,33] were added variationally to the total energy for all systems. In view of the fact that all systems investigated in this work show a large HOMO−LUMO gap, a spin-restricted formalism was used for all calculations. No symmetry constraints were used.

Acknowledgment. We are grateful to the Korea Research Foundation (Grant No. KRF-2002-015-CP0200) for their financial support.

Supporting Information Available: Crystallographic data (excluding structure factors) for the structures **2a**, **6**, **8**, and **9**·2C_7H_8 reported in this paper and listings giving optimized geometries of the crucial structures reported (Cartesian coordinates, in Å); crystallographic data are also available in electronic form as CIF files. This material is available free of charge via the Internet at http://pubs.acs.org.

OM034194D

(20) Baerends, E. J.; Ellis, D. E.; Ros, P. *Chem. Phys.* **1973**, *2*, 41.
(21) Baerends, E. J.; Ros, P. *Chem. Phys.* **1973**, *2*, 52.
(22) Ravenek, W. In *Algorithms and Applications on Vector and Parallel Computers*; te Riele, H. J. J., Dekker, T. J., van de Horst, H. A., Eds.; Elsevier: Amsterdam, The Netherlands, 1987.
(23) te Velde, G.; Baerends, E. J. *J. Comput. Chem.* **1992**, *99*, 84.
(24) Boerrigter, P. M.; te Velde, G.; Baerends, E. J. *Int. J. Quantum Chem.* **1988**, *33*, 87.
(25) Versluis, L.; Ziegler, T. *J. Chem. Phys.* **1988**, *88*, 322.
(26) Snijders, J. G.; Baerends, E. J.; Vernoijs, P. *At. Nucl. Data Tables* **1982**, *26*, 483.
(27) Vernoijis, P.; Snijders, J. G.; Baerends, E. J. *Slater Type Basis Functions for the Whole Periodic System*; Internal Report (in Dutch); Department of Theoretical Chemistry, Free University: Amsterdam, The Netherlands, 1981.
(28) Krijn, J.; Baerends, E. J. *Fit Functions in the HFS Method*; Internal Report (in Dutch); Department of Theoretical Chemistry, Free University: Amsterdam, The Netherlands, 1984.
(29) Vosko, S. H.; Wilk, L.; Nusair, M. *Can. J. Phys.* **1980**, *58*, 1200.
(30) Becke, A. *Phys. Rev. A* **1988**, *38*, 3098.
(31) (a) Perdew, J. P. *Phys. Rev. B* **1986**, *34*, 7406. (b) Perdew, J. P. *Phys. Rev. B* **1986**, *33*, 8822.
(32) Snijders, J. G.; Baerends, E. J. *Mol. Phys.* **1978**, *36*, 1789.
(33) Snijders, J. G.; Baerends, E. J.; Ros, P. *Mol. Phys.* **1979**, *38*, 1909.